ARTICLES
PUBLISHED ONLINE: 22 MAY 2011 | DOI: 10.1038/NGEO1157

nature geoscience

Rapid tremor reversals in Cascadia generated by a weakened plate interface

Heidi Houston*, Brent G. Delbridge, Aaron G. Wech and Kenneth C. Creager

Slow slip along the plate interface at subduction zones can generate weak seismic tremor in a quasi-periodic process called episodic tremor and slip. This process differs in character from regular earthquake rupture and can release stresses that build up on the deep plate interface. Here we analyse the spatial and temporal evolution of the five largest episodic tremor and slip events between 2004 and 2009 in northern Washington on the Cascadia subduction zone. We find that the events are similar, but not identical because they initiate in different locations and propagate along the plate interface at different average speeds of 7 to 12 km per day. Our analysis reveals that tremor can migrate rapidly back, away from the region where tremor and slip are advancing, through parts of the plate interface that have just ruptured in the past three days. These rapid tremor reversals propagate backwards for tens of kilometres at speeds that are 20 to 40 times faster than the relatively slow, steady advance of episodic tremor and slip. Our observations suggest that once the plate interface is weakened by the initial advance of episodic tremor and slip, it allows stresses to induce slip more easily or fluid pressure waves to migrate back more rapidly, generating rapid tremor reversals.

Episodes of weak seismic radiation (termed tremor) and slow slip occur together in a coupled process that has been detected recently in several subduction zones[1–5]. The episodes are called Episodic Tremor and Slip (ETS) in Cascadia and Slow Slip Events (SSE) in Japan. Reference 6 provides a recent review of Cascadia-wide ETS. In contrast with regular earthquakes, tremor signals exhibit low amplitudes, long durations, and emergent character. In northern Washington, ETS manifests in SSE that last 2–4 weeks, extend over 150 km along strike of the Cascadia subduction zone, and involve a moment release equivalent to a M6.4 to 6.8 earthquake. Recurring every 12–15 months, they are tantalizingly near-periodic in occurrence, compared with the aperiodicity of regular earthquakes.

The nature and location of ETS has important implications for the mechanics and seismic hazards of subduction zones. The source character and scaling of tremor seem distinct from regular earthquakes[7]. Furthermore, the process propagates at speeds much slower than regular earthquakes. These aspects of ETS pose a major challenge to understanding its physics. The total moment release in the northern Cascadia ETS is a large fraction of that accumulated over an inter-ETS period[8,9]. Thus, stress accumulation in the ETS portion of subduction zones is probably much less than that in the locked zone, which lies updip. In Cascadia, the locked zone is known to be capable of M9 earthquakes[10]. Therefore, the location of the ETS region may help to delineate the lower bound of the zone likely to slip seismically in great megathrust earthquakes[9]. Furthermore, episodic stress transfer by ETS adjacent to the locked zone points to a potential role in triggering large megathrust earthquakes, and motivates tremor-monitoring efforts.

Here, we compare the behaviour of five large ETS in northern Washington and report a new phenomenon, in which tremor travels rapidly back across a region through which the ETS has very recently ruptured. We then discuss three distinct ETS propagation processes with different velocities, all of which are anomalously slow compared with seismic velocities.

Tremor catalogues

We analyse tremor location catalogues for the July 2004, September 2005, January 2007, and May 2008 ETS in northern Washington[8], as well as the more recent May 2009 event[11]. These are derived using a waveform envelope cross-correlation and clustering algorithm[12]. Together, the five catalogues represent ∼110 days of relatively strong tremor and ∼16,000 locations.

The location procedure yields epicentral locations with estimated errors of about ±8 km, but depth determinations are highly uncertain[12]. Therefore, we focus mainly on epicentral locations. However, we also consider the implications if all the tremor is located on the plate interface, and for that purpose assume that the interface is described by a 3D model of the subducting plate[13]. Several recent results support the concept that the majority of tremor concentrates on the plate interface between the over-riding and down-going plates[14–17], although evidence also suggests some tremor occurs throughout a large volume above the interface[18]. As discussed below, the former concept seems more consistent with the occurrence of Rapid Tremor Reversals (RTR).

Comparison of ETS space–time evolution

To assess and compare along-strike ETS propagation velocities, we projected the tremor epicentres from the five episodes onto a straight line, obtained by fitting the epicentres of the 2007 ETS (Fig. 1), which is the most spatially extensive of the five ETS. Epicentres from all five episodes are projected onto this common along-strike line, so that the along-strike propagation behaviour can be readily examined.

The left panels of Fig. 1 show maps of the tremor locations during the five ETS, whereas distance along the projection line (black line in the maps) versus time is shown on the right. Epicentres are colour-coded by depth to the plate interface model[13] below, with red to purple to blue denoting increasing depth.

Although the space–time evolution is similar for the five ETS, they are not exact replicas. All five episodes share the

Department of Earth and Space Sciences, University of Washington, Johnson Hall Rm-070, 4000 15th Avenue NE, Seattle, Washington 98195-1310, USA. *e-mail: Heidi.Houston@gmail.com.

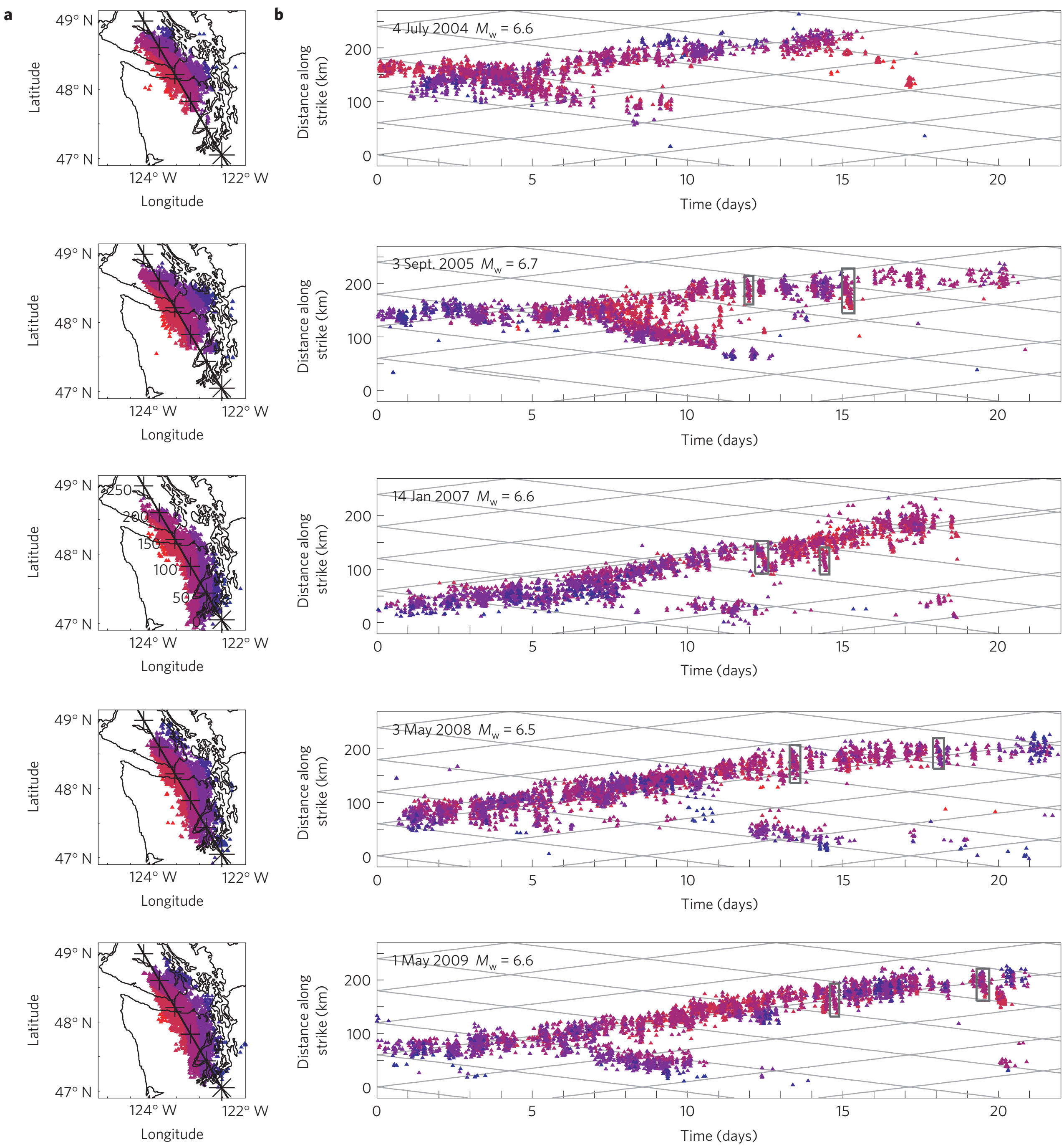

Figure 1 | Detailed space–time evolution of five ETS. a, Maps of five major ETS, with epicentral tremor locations colour-coded by depth above the modelled plate interface[13], with red to purple to blue denoting increasing depth (depth ranges 25–30, 30–35, 35–40, 40–45, 45–50, and 50–55 km). The black line is an estimate of the along-strike direction of overall ETS propagation, obtained by fitting the 2007 ETS. The star marks 0 km along the line and + symbols mark 50 km increments. **b**, Time versus distance projected along the strike line (black line in **a**). Tremor locations are colour-coded as in **a**. Time is measured from midnight GMT on the dates given. Grey boxes indicate the RTR selected for analysis and shown in Fig. 3.

tendency to propagate primarily northwestward, but initiated from three different spots along strike (Fig. 2). Each episode also shows some degree of southward propagation of tremor from a location just south of the initiation point, but this feature is more developed in the 2005 and 2009 catalogues. The common features, particularly the tendency to propagate mainly northwestward, suggest the influence of permanent aspects of the plate interface, such as geometry.

In interpreting the features of these catalogues, some limitations should be considered. The catalogues were derived from different station sets, depending on data, station, and network availability over the pertinent time periods. At the northern end of our study area, poor station availability on Vancouver Island during the period of this study could produce an apparent slowdown in ETS propagation as tremor moved northwest out of our area of station coverage. However, this artefact is appreciable only during the 2005 ETS, based on comparison with the tremor catalogue of the Canadian Pacific Geoscience Center. In particular, the marked slowdown during the 2008 ETS seems to be a real feature, as the ETS almost stalled under southern Vancouver

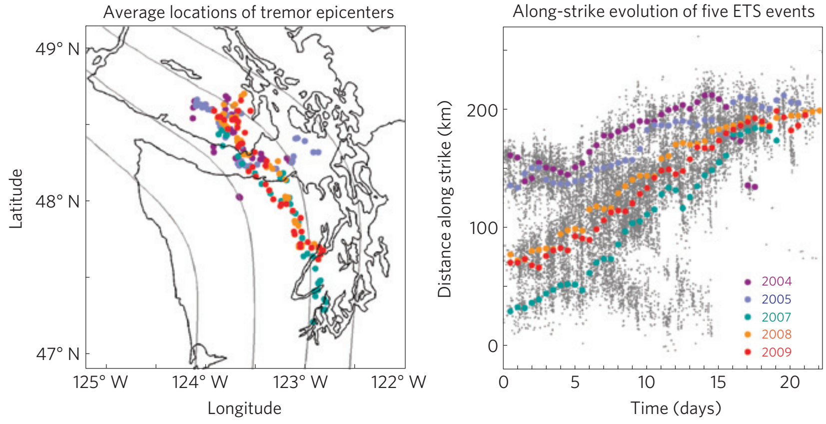

Figure 2 | Comparison of the average space–time evolution of five ETS. (Left) Average tremor locations in moving windows of 24-h duration. In many instances, the different ETS seem to travel along the same paths on the plate interface. (Right) Time versus distance along strike, highlighting the variations in propagation velocity and initiation location between events. The strike line is the same as in Fig. 1. Grey points show all tremor. Tremor in the south-going arms was removed from the averaging process to focus on the primary progression of ETS in a northwesterly direction.

Island then sped up again as it propagated further north along the island[19]. At the southern end of our study area, a catalogue encompassing a larger region, available for a more limited time period, shows that tremor continued over 100 km farther south in 2007 and 2008, but its behaviour in 2004, 2005, and 2009 is unknown. Nevertheless, much can be inferred from the tremor that was located.

The initial portions of the 2004 and 2005 ETS are distinctive in that tremor stays near the initiation point for up to 8 days before the usual ETS along-strike migration begins. A further peculiarity is that the 2004 tremor initiates in two distinct locations separated by 60 km and 24 h. In general, after initiation, a given site along strike typically continues to host tremor for four to five days.

Although an analysis of tremor amplitude is beyond the scope of this paper, amplitude data from array observations of the 2004, 2005, and 2007 ETS events[20], show a roughly linear increase in tremor amplitude during the first five days of each of those events. Perhaps tremor and slip initiate at a point and expand over the plate interface such that the area increases linearly in time (and the radius increases as the square root of time) until it reaches the width of the ETS tremor region, then continues to expand linearly in area, but only in the along-strike direction such that the propagation front is then linear and moving more rapidly along strike.

Figure 1 also shows the general tendency on a large scale for tremor epicentres to propagate in a somewhat updip direction during these ETS, as they cross the broad arch in the subducting plate under the NE Olympic Peninsula, an arch believed to be created by the reverse curvature of the subduction zone[21]. On a smaller scale, several cases in which tremor epicentres start downdip (bluer symbols) and migrate in an updip direction (redder symbols) are visible—for example, the first seven days of 2005, as well as the south-going arms of 2005 and 2009.

Along-strike propagation velocities can be estimated by comparing the slopes in the time-distance plots to the grey reference lines in Fig. 1b, which show a velocity of $\pm 7\,\mathrm{km\,d^{-1}}$. The velocities of ETS advancement reported here are broadly consistent with the generally cited velocity of about $10\,\mathrm{km\,d^{-1}}$ for Cascadia and Japan[8,22], but our analysis is able to reveal significant variations (Figs 1 and 2). Along-strike tremor propagation velocities achieved during the five episodes vary both during a specific ETS and for different ETS—from $7\,\mathrm{km\,d^{-1}}$ to $12\,\mathrm{km\,d^{-1}}$ averaging over intervals of at least three days. Higher along-strike velocities are seen for the 2007 ETS, later in an episode, and in the southward propagating arms of the episodes (Fig. 1).

Rapid Tremor Reversals

Close scrutiny of the time–distance plots in Fig. 1 reveals a new feature of tremor organization—streak-like clusters of tremor that propagate rapidly back from the front of the advancing tremor through the region that has already experienced tremor, termed Rapid Tremor Reversals (RTR). These are visible on Fig. 1 as nearly vertical lines of tremor that slant steeply in the opposite direction to the prevailing tremor propagation. Although the exact slopes of these features depend on the projection, as long as the strike of the projection line lies within a few tens of degrees of the actual advance of the ETS, the existence of these features indicates tremor moving in the opposite direction to the slow overall advance of ETS.

Grey boxes on the right-hand part of Fig. 1 show eight of these RTR that were selected for further analysis. Figure 3 shows the epicentral locations of the selected streaks, with blue dots representing tremor at early times and green dots indicating later times. In most cases the regions they occupy are elongated. The durations of the RTR range from 2.5 to 11 h. Although the relatively prominent RTRs studied here tend to occur near the Straits of Juan de Fuca, RTRs occur in other regions as well, including on the south-going arm of the 2005 ETS, as well as in the 2009 ETS near Portland (for example, 1 September, 2009). A clear case of rapid forward propagation of tremor occurred near and just before the 15 May, 2009 RTR.

We estimate the propagation velocity of the RTRs, not from the slopes on Fig. 1, but by fitting straight lines and flat planes to RTR epicentres versus time (see Supplementary Information and Figure). Estimates of their velocities are given on Fig. 3 and range from 160 to $400\,\mathrm{km\,d^{-1}}$ (7 to $17\,\mathrm{km\,h^{-1}}$). Thus, RTR tremor propagates 'backwards' 20 to 40 times faster than ETS advances forward. These velocities are intermediate between those of the slow along-strike progression of ETS (7 to $12\,\mathrm{km\,d^{-1}}$) and the recently observed rapid streaks of tremor that zip nearly up- and downdip at speeds of 25 to $100\,\mathrm{km\,h^{-1}}$ (ref. 23).

The relationship between RTRs and the overall ETS process has implications for temporal changes in the state of the plate interface and its mechanical properties. Within the resolution of these locations, all the RTR regions have hosted tremor during the three days before RTR initiation (grey dots in Fig. 3). Thus, if the slip and tremor fronts are roughly coincident, the RTR regions have already been ruptured in ETS. One interpretation is that fluid pressure waves may propagate back along the previously ruptured plate interface more rapidly than they can advance. There have been several observations of tremor triggered by large surface waves in regions that have recently ruptured in an ETS (ref. 24). This suggests

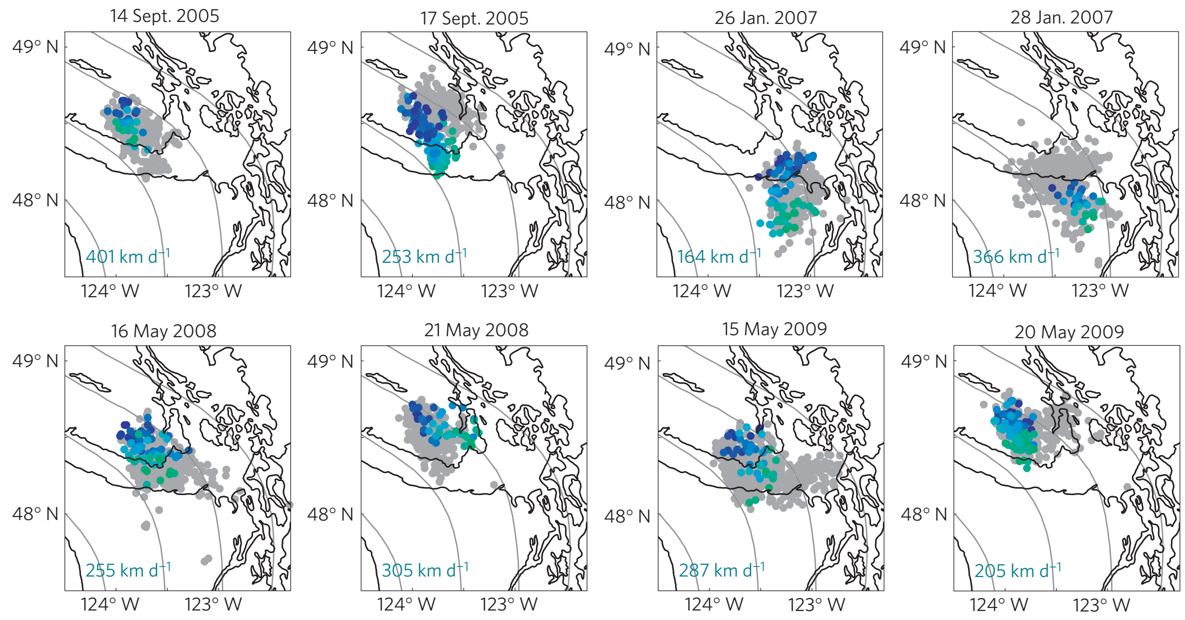

Figure 3 | RTR location and progression. Maps of the eight selected RTR in grey boxes in Fig. 1. Blue dots represent epicentres at early times during each RTR, green later times. Dates and estimated velocities of propagation of the RTR are given. Grey dots show the tremor locations during the previous three days. Thin grey lines show contours of the subducting plate at 20, 30, 40, and 50 km depth from a model of the plate interface[13].

that tremor sources on the plate interface are more sensitive to stress changes shortly after ETS has passed through, even though the ETS lowered the average ambient shear stress. This greater sensitivity could play a role in the rapid propagation of RTR. If tremor sources are considered as sticky asperities surrounded by slow slip, then depending on the relative slip of the asperities and their surroundings, some may sustain increased stress concentrations following the passage of the main ETS front.

The location of RTRs with respect to the advancing ETS front is relevant for models of the process. RTR mostly initiate near the ETS front, but a few initiate up to 30 km behind it. The advancing ETS seems to maintain a fairly consistent along-strike extent of about 20–40 km (Fig. 1b), owing partly to location scatter. Most of the RTRs clearly travel back beyond the currently active ETS region, and occasionally up to 30 km beyond it. The rhythmic 'pulsing' of the ETS evident in Figs 1 and 2 may be owing to tidal stressing, daily interference in detection from cultural noise (particularly that in Fig. 2), and the abrupt advance of 'tremor bands' (ref. 25). RTRs seem to occur preferentially near the Straits of Juan de Fuca, which is also where the pulsing becomes more pronounced (Fig. 1b). This suggests that tidal stressing could play a role in the generation of RTRs, particularly as the plate interface seems more sensitive following ETS.

The existence of RTRs supports the concept that most tremor is generated on the plate interface. The direction of propagation of the RTR back along strike and usually slightly updip is understandable in the context of tremor located on a plate interface, which may change state or condition after the passage of ETS. It is less explicable in a context with most tremor located throughout a large volume above the plate interface. Such a situation would provide no obvious reason that tremor would propagate rapidly through an elongated zone well above the plate interface in the opposite direction to the overall slow steady advance of ETS.

Comparison of ETS, RTR, and streak velocities

Tremor behaviour with three different characteristic propagation velocities and geometries has now been observed in the northern Washington ETS events (Fig. 4). We have shown here that the overall along-strike advance of ETS takes place at 7–12 km d^{-1}, and that tremor in RTRs travels in roughly the opposite direction at 160–400 km d^{-1}. An even faster mode of tremor propagation has been observed in northern Washington[23]. Waveforms from a dense array were beamformed to reveal 'streaks' of tremor propagating back and forth parallel to the plate convergence direction (nearly up- and downdip) over tens of km and for tens of minutes with velocities of 25–100 km h^{-1} (ref. 23). Similar rapid streaking of tremor has been seen in Japan[26]. The velocities of these three modes of tremor propagation, although different, are all much slower than seismic speeds, with even the fastest process, streaking, about 2.5 orders of magnitude slower than the S-wave propagation speed (Fig. 4c).

The physical processes operative during ETS are unknown. A key question involves the factors that control the advance of ETS along strike, as well as the propagation of RTRs and streaking. Two general mechanisms that have been considered involve stress transfer from prior slip and the migration or diffusion of fluid or fluid pressure. As discussed below, the slow speeds of all three ETS processes mentioned above relative to seismic wave velocities in rock or fluid raise issues for the interpretation of ETS propagation through stress transfer. At the same time, the rapid speeds of the ETS processes relative to fluid migration and diffusion speeds, if typical crustal permeabilities and diffusivities apply, complicate an interpretation that one or more of the processes is driven by fluid migration. However, rapid fluid migration through cm-scale conduits has been proposed as one of several potential mechanisms for streaking[23].

Figure 4b suggests that the length and timescales of the individual RTR, together with the streaks, seem to follow a diffusional relation (one in which distance travelled is proportional to the square root of time); the ETS itself propagates three times slower than predicted by the relation. Perhaps the advancing ETS fractures or otherwise weakens the plate interface[27] so that the faster processes (streaks and RTR), which occur in already slipped or slipping regions, can occur in a more permeable setting. However, the RTR propagation tends to proceed at a roughly constant speed, rather than slow down in a diffusional manner (Supplementary Fig. S1). The diffusivity implied in Fig. 4b is very large, nearly 10^4 m^2 s^{-1}, which is about two orders of magnitude larger than even the largest

NATURE GEOSCIENCE DOI: 10.1038/NGEO1157

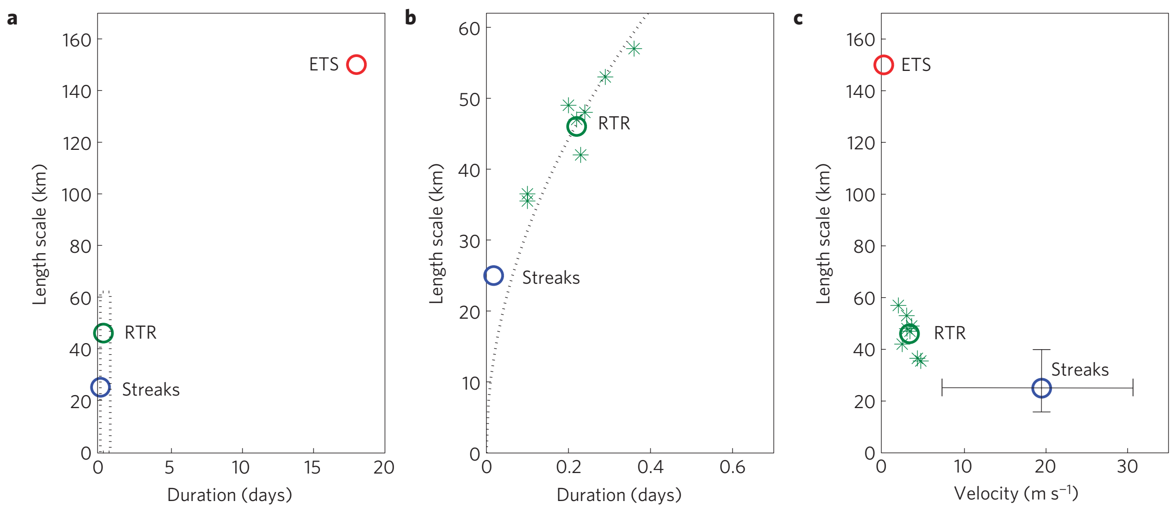

Figure 4 | Comparison of length scales, timescales, and propagation velocities of the three ETS propagation modes: along-strike advance of ETS, RTR, and rapid up- and downdip streaking. a, Duration versus length scale of processes. Dots represent average values of the length and durations. **b**, A closer look at data inside the dotted box in **a**.Green asterisks represent the eight RTR. The dotted line shows a diffusional relationship between length and duration, with diffusivity of 9,000 $m^2 s^{-1}$. **c**, Propagation velocity of the process versus length scale of the process. Error bars on the streak symbol show the range of 90% of the streaks[23].

crustal estimates (Table 1 of ref. 28). Nevertheless, a recent analysis of tremor migration in Japan found that tremor often migrates in a diffusive manner with a diffusivity of $\sim 10^4$ $m^2 s^{-1}$ (ref. 29), although the physical significance of this remains unclear.

Stress transfer occurs at seismic speeds. For the much more slowly propagating processes of ETS, RTR and streaks, a simple calculation illustrates the long delays between the arrival of stress at a given location, and seismic failure there (see Supplementary Information). For the characteristic propagation speeds of 7 km d^{-1}, 200 km d^{-1}, and 50 km h^{-1}, for ETS, RTR, and streaking, respectively, the delays associated with a stress transfer distance of 1 km (that is, stress generated by slip 1 km away) would be 12,000, 430, and 72 s, respectively. However, during triggering of tremor by strong surface waves of large distant earthquakes, the delay between maximum shear stresses and tremor maxima is at most 2–3 s and often not resolvably different from zero[30].

However, although the transfer of stress occurs at seismic speeds, a slowly propagating stress increase would be generated in front of a slowly propagating creep transient, as could be triggered by a stress perturbation on a creeping fault[31]. Furthermore, rate-and-state models produce creep transients that propagate faster where the background slip velocity is faster (that is, during and shortly after ETS rupture through a region) and may be consistent with the three tremor processes. Our observations of RTRs, including their occurrence in previously ruptured regions, and their origination near the ETS front and propagation back beyond it, fit within the context of rate-and-state models of such creep waves[32]. Such models predict a scaling between widths and velocities of creep waves that is roughly consistent with the three observed modes of tremor propagation[32] (that is, advance of ETS fronts, RTRs, and streaking). Furthermore, other models of ETS propagation must be able to address the observations presented here, which supply powerful constraints.

A more general consideration is that if tremor propagation is mainly controlled by stress transfer, propagation velocities should accelerate as slip accumulates, whereas if tremor propagation is driven mainly by fluid diffusion, velocities would be expected to decelerate. In actuality, during the large ETS in northern Washington, neither acceleration nor deceleration dominate. The relatively constant velocities of these major ETS might suggest the operation of a renewal process, for example, renewal of fluid pressure as the ETS propagates, as might occur if the slip promotes generation of fluids, which promote further slip, but again diffuse away.

The characterization of diverse tremor propagation processes may hold the key to the identification of the physical environment and mechanisms of ETS.

Methods

The tremor location catalogues used in this study are determined with a waveform envelope cross-correlation and clustering algorithm[12]. We bandpass filter vertical-component regional network seismograms from 1 to 8 Hz, compute envelope functions, and then low-pass filter at 0.1 Hz. Locations are determined from the cross-correlation of 5-min. windows. The windows are overlapped by 2.5 mins so that the maximum number of tremor detections per hour is 24. In a given 5-min. window, the location algorithm will find tremor in only one location, even though tremor may be occurring in two or more locations, as, for example, in bilaterally propagating ETS (see Supplementary Information).

We projected epicentres from all five ETS episodes onto a common along-strike line, so that the along-strike propagation behaviour could be readily examined. The straight line onto which the tremor epicentres were projected was obtained by fitting the epicentres of the 2007 ETS (Fig. 1a), which is the most spatially extensive of the five ETS. To reduce the effects of outliers, we determined this line using an L1 norm that minimizes the sum of the orthogonal distances of each tremor epicentre from the line. The resulting line strikes 41° west of north and is shown in the left panels of Fig. 1. The along-strike propagation velocities along the projection line would decrease only slightly for small ($<20°$) deviations from the optimal, best-fitting line.

Received 29 December 2010; accepted 18 April 2011; published online 22 May 2011

References

1. Obara, K. Nonvolcanic deep tremor associated with subduction in southwest Japan. *Science* **296,** 1679–1681 (2002).
2. Rogers, G. & Dragert, H. Episodic tremor and slip on the Cascadia subduction zone: The chatter of silent slip. *Science* **300,** 1942–1943 (2003).
3. Schwartz, S. Y. & Rokosky, J. M. Slow-slip events and seismic tremor at circum-Pacific subduction zones. *Rev. Geophys.* **45,** RG3004 (2007).
4. Peterson, C. L. & Christensen, D. H. Possible relationship between nonvolcanic tremor and the 1998–2001 slow slip event, south central Alaska. *J. Geophys. Res.* **114,** B06302 (2009).
5. Song, T. A. *et al.* Subducting slab ultra-slow velocity layer coincident with silent earthquakes in southern Mexico. *Nature* **324,** 502–506 (2009).
6. Gomberg, J. The Cascadia 2007 and Beyond Working Group. Slow-slip phenomena in Cascadia from 2007 and beyond: A review. *Geol. Soc. Am. Bull.* **122,** 963–978 (2010).
7. Ide, S., Beroza, G. C., Shelly, D. R. & Uchida, T. A scaling law for slow earthquakes. *Nature* **447,** 76–79 (2007).

8. Wech, A. G., Creager, K. C. & Melbourne, T. I. Seismic and geodetic constraints on Cascadia slow slip. *J. Geophys. Res.* **114,** B10316 (2009).
9. Chapman, J. S. & Melbourne, T. I. Future Cascadia megathrust rupture delineated by episodic tremor and slip. *Geophys. Res. Lett.* **36,** L22301 (2009).
10. Atwater, B. F. Evidence for great Holocene earthquakes along the outer coast of Washington State. *Science* **236,** 942–944 (1987).
11. Wech, A. G. Interactive tremor monitoring. *Seismol. Res. Lett.* **81,** 664–669 (2010).
12. Wech, A. G. & Creager, K. C. Automatic detection and location of Cascadia tremor. *Geophys. Res. Lett.* **35,** L20302 (2008).
13. McCrory, P. A., Blair, J. L., Oppenheimer, D. H. & Walter, S. R. Depth to the Juan de Fuca slab beneath the Cascadia subduction margin: A 3-D model for sorting earthquakes: U.S. Geological Survey Data Series DS-91, 1 CD-ROM, Version 1.2, 2006.
14. Shelly, D. R., Beroza, G. C., Ide, S. & Nakamula, S. Low-frequency earthquakes in Shikoku, Japan, and their relationship to episodic tremor and slip. *Nature* **442,** 188–191 (2006).
15. Ide, S., Shelly, D. R. & Beroza, G. C. Mechanism of deep low frequency earthquakes: Further evidence that deep non-volcanic tremor is generated by shear slip on the plate interface. *Geophys. Res. Lett.* **34,** L03308 (2007).
16. LaRocca, M. *et al.* Cascadia tremor located near the plate interface constrained by S minus P wave times. *Science* **323,** 620–623 (2009).
17. Brown, J. R. *et al.* Deep low-frequency earthquakes in tremor localize to the plate interface in multiple subduction zones. *Geophys. Res. Lett.* **36,** L19306 (2009).
18. Kao, H. *et al.* A wide depth distribution of seismic tremors along the northern Cascadia margin. *Nature* **436,** 841–844 (2005).
19. Dragert, H., Wang, K. & Kao, H. On the temporal evolution of an ETS event along the Northern Cascadia margin (abstract). *Seismol. Res. Lett.* **81,** 337 (2010).
20. Rubenstein, J. L., La Rocca, M., Vidale, J. E., Creager, K. C. & Wech, A. G. Tidal modulation of non-volcanic tremor. *Science* **319,** 186–189 (2008).
21. Chiao, L-Y. & Creager, K. C. in *The Cascadia Subduction Zone and Related Subduction Systems—Seismic Structure, Intraslab Earthquakes and Processes, and Earthquake Hazards,* USGS Open File Report 02-328 and Geological Survey of Canada Open File 4350 (eds Kirby, S.H. & Wang, K.) 47–54 (2002).
22. Obara, K. & Sekine, S. Characteristic activity and migration of episodic tremor and slow-slip events in central Japan. *Earth Planets Space* **61,** 853–862 (2009).
23. Ghosh, A. *et al.* Rapid, continuous streaking of tremor in Cascadia. *Geochem. Geophys. Geosyst.* **11,** Q12010 (2010).
24. Gomberg, J. Lessons from (triggered) tremor. *J. Geophys. Res.* **115,** B10302 (2010).
25. Ghosh, A. *et al.* Tremor bands sweep Cascadia. *Geophys. Res. Lett.* **37,** L08301 (2010).
26. Shelly, D. R., Beroza, G. C. & Ide, S. Complex evolution of transient slip derived from precise tremor locations in western Shikoku, Japan. *Geochem. Geophys. Geosyst.* **8,** Q10014 (2007).
27. Audet, P., Bostock, M. G., Christiansen, N. I. & Peacock, S. M. Seismic evidence for overpressured subducted oceanic crust and megathrust fault sealing. *Nature* **457,** 76–78 (2009).
28. Ingebritsen, S. E. & Manning, C. E. Permeability of the continental crust: Dynamic variations inferred from seismicity and metamorphism. *Geofluids* **10,** 193–205 (2010).
29. Ide, S. Striations, duration, migration and tidal response in deep tremor. *Nature* **466,** 356–359 (2010).
30. Rubenstein, J. L *et al.* Seismic wave triggering of nonvolcanic tremor, episodic tremor and slip, and earthquakes on Vancouver Island. *J. Geophys. Res.* **114,** B00A01 (2009).
31. Perfettini, H. & Ampuero, J-P. Dynamics of a velocity strengthening fault region: Implications for slow earthquakes and postseismic slip. *J. Geophys. Res.* **113,** B09411 (2008).
32. Ampuero, J-P. Migration patterns and scaling laws of slow slip and tremor resulting from the collective behavior of fault asperities mediated by transient creep. *EOS Trans. AGU* **91** (Fall Meet. Suppl.) Abstr. no S13D-03, 2010.

Acknowledgements

We are grateful for enlightening discussions with A. Rubin and J-P. Ampuero and helpful suggestions from D. Shelly for improving this manuscript. We thank H. Kao for supplying the tremor catalogue of the Pacific Geoscience Center for purposes of comparison. This work was supported by NSF grant EAR-0911759.

Author contributions

H.H. designed the study and wrote the paper. B.G.D. and H.H. analysed the data and made the figures. A.G.W. and K.C.C. determined the tremor locations. H.H., B.G.D. and K.C.C. were involved in the interpretation.

Additional information

The authors declare no competing financial interests. Supplementary information accompanies this paper on www.nature.com/naturegeoscience. Reprints and permissions information is available online at http://www.nature.com/reprints. Correspondence and requests for materials should be addressed to H.H.